PIOTR GAJEWSKI, KRZYSZTOF PIEŃKOWSKI[*]

APPLICATION OF DIRECT TORQUE AND POWER CONTROL TO THE WIND TURBINE SYSTEM WITH PMSG

ZASTOSOWANIE METODY BEZPOŚREDNIEGO STEROWANIA MOMENTEM I MOCĄ ELEKTROWNI WIATROWEJ Z PMSG

Abstract

The paper presents the wind energy conversion system with a direct driven Permanent Magnet Synchronous Generator (PMSG). The system consists of a wind turbine with a PMSG, the Machine Side Converter (MSC) and the Grid Side Converter (GSC). In order to control the MSC, the Direct Torque Control with Space Vector Modulation (DTC-SVM) has been applied. To achieve the maximum power from the wind turbine, the Maximum Power Point Tracking algorithm has been used. In order to control the GSC, the Direct Power Control with Space Vector Modulation (DPC-SVM) has been used. In order to obtain high power quality, the LCL grid filter has been used in the GSC. The performed simulation studies confirmed the high effectiveness of the Direct Torque and Direct Power control method.

Keywords: wind turbine, PMSG, MPPT, DTC, DPC, LCL grid filter, simulation studies

Streszczenie

Przedstawiono przekształtnikowy układ elektrowni wiatrowej z generatorem synchronicznym o magnesach trwałych (PMSG). System składa się z turbiny wiatrowej, sprzężonej bezpośrednio z generatorem PMSG, przekształtnika maszynowego (MSC) oraz przekształtnika sieciowego (GSC). Do sterowania MSC zastosowano metodę bezpośredniego sterowania momentem (DTC). W celu wykorzystania maksymalnej mocy turbiny wiatrowej zastosowano algorytm MPPT. Do sterowania GSC zastosowano metodę bezpośredniego sterowania mocą (DPC). Wykonane badania symulacyjne potwierdziły dobre właściwości rozpatrywanych metod sterowania.

Słowa kluczowe: turbina wiatrowa, PMSG, MPPT, DTC, DPC, filtr sieciowy LCL

[*] M.Sc. Eng. Piotr Gajewski, D.Sc. Ph.D. Eng. Krzysztof Pieńkowski, Department of Electrical Machines, Drives and Measurements, Faculty of Electrical Engineering, Wroclaw University of Science and Technology.

1. Introduction

The wind turbine technology is still one of the most promising renewable energy technologies [1, 2, 5, 6]. Nowadays, the Voltage Source Converters (VSC) are mostly used in wind energy conversion systems (WECS). Specifically, the back-to-back converters for direct driven wind generation system with Permanent Magnet Synchronous Generator (PMSG) have been widely applied [2, 5, 8]. A typical configuration of a back-to-back converter system is illustrated in Fig. 1.

The wind turbine is directly coupled to the PMSG generator. The stator winding of PMSG is connected to a full-scale, back-to-back Voltage Source Converter system. This converter system is composed of the Machine Side Converter (MSC) and the Grid Side Converter (GSC). The GSC is connected to the AC grid through the LCL grid filter. This type of converter allows to achieve full control over the active and reactive instantaneous power delivered to the AC grid [15]. Moreover, the back-to-back converter provides the decoupling between the PMSG and the AC grid.

The high reliability of a variable speed wind turbine system with a direct driven PMSG can be improved significantly in comparison to a doubly-fed induction generator with a gearbox [1, 15]. The advantages of the direct driven PMSG generator compared to a generator with a gearbox increased reliability and the reduction of the weight of the whole system. The results of directly coupling the generator with a wind turbine allow for the elimination of a gearbox installation and a reduction of maintenance costs [8, 15].

The objective of this paper is to analyze the wind energy conversion system with the direct driven PMSG. In the considered control system of both converters, the vector control methods have been applied.
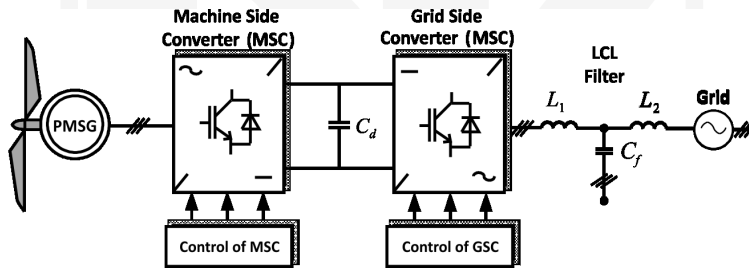

Fig. 1. Configuration of variable speed wind turbine system with direct driven PMSG, back-to-back converter system and LCL grid filter

In the control system of the MSC, the Direct Torque Control with Space Vector Modulation (DTC-SVM) method has been used. Direct Torque Control has many advantages, such as its simple structure and fast dynamic response [2, 5, 8, 16, 17]. However, in order to obtain the maximum power from the wind turbine, the Maximum Power Point Tracking (MPPT) algorithm has been used. Additionally, in order to prevent the possibility of mechanical damage of the wind turbine and in order to achieve the limitation of maximum power, the pitch angle scheme is included. In order to control the GSC, the Direct Power

Control with Space Vector Modulation (DPC-SVM) method has been used. In order to obtain high power quality and to reduce the current harmonic in the output of the GSC, the LCL grid filter has been applied [7, 11, 12].

This paper is structured in 9 sections. In Section 1, the principle of development of the wind energy conversion system has been presented. Section 2 and 3 describe the model of wind turbine and the model of the PMSG. Section 4 gives the description of the pitch angle control and the MPPT algorithm. Then, the Direct Torque Control of the PMSG is studied in Section 5. Section 6 presents a control strategy of Direct Power Control of the GSC. Section 7 describes the principle of the LCL grid filter design. Simulation results of the considered wind energy conversion system are provided in Section 8. Finally, the research conclusions are presented in section 9.

2. Wind Turbine Model

The mechanical output power from a wind turbine depends on the rotor swept area, wind speed, power coefficient of wind turbine and density of air. The average total amount of power captured by the wind turbine P_t can be expressed through the following relation [2–4, 14, 15]:

$$P_t = \frac{1}{2}\rho A C_p\left(\lambda,\beta\right)v_w^3 \tag{1}$$

where:

ρ – air density,
$A = \pi R^2$ – area swept by the rotor blades,
R – radius of the turbine blade,
C_p – power coefficient of the wind turbine,
λ – tip speed ratio,
β – blade pitch angle,
v_w – wind speed.

The power coefficient C_p is dependent on the design parameters of the wind turbine, tip speed ratio λ and pitch angle β, respectively. The tip speed ratio is defined as a ratio between the speed of the blade tip (v_{tip}) to wind speed v_w.

$$\lambda = \frac{v_{tip}}{v_w} = \frac{\omega_m R}{v_w} \tag{2}$$

where:

ω_m – angular speed of turbine rotor.

The characteristic of $C_p(\lambda, \beta)$ can be approximated by non-linear function [2, 14, 15]:

$$C_p(\lambda,\beta) = 0.5176\left(\frac{116}{\lambda_i} - 0.4\beta - 5\right)\cdot e^{\left(-\frac{21}{\lambda_i}\right)} + 0.0068\lambda \tag{3}$$

where:

λ_i – is variable, which is a function of λ and β and is defined as:

$$\lambda_i = \left(\frac{1}{\lambda + 0.08} - \frac{0.035}{\beta^3 + 1}\right)^{-1} \tag{4}$$

The typical power characteristics of a wind turbine operating at different wind speeds have been shown in Fig. 2 [14, 15]. These characteristics represent the wind turbine power curves as a function of the rotor angular speed ω_m at various wind speeds v_w. From this Figure, it can be stated that, for each wind speed, there is a maximum power point that the turbine could extract maximum power. This condition of Maximum Power Point Tracking is fulfilled, when the turbine operates at optimal rotor speed ω_{opt}. Hence, it follows that, in order to obtain the maximum power from the wind, the turbine must be operated at optimal tip speed ratio λ_{opt}.
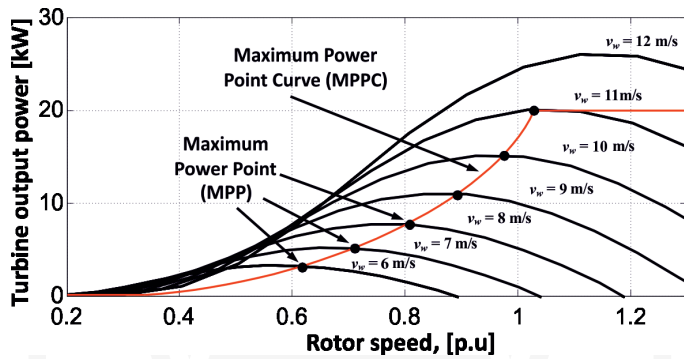

Fig. 2. Characteristics of the wind turbine power as function of rotor angular speed at various wind speeds

The mechanical output power from the wind turbine can be written using equations (1) and (2), so the trajectory of the Maximum Power Point Curve (MPPC) represents a power curve, which can be described by [14, 15]:

$$P_{MPPT} = K_{opt}\omega_{opt}^3 \tag{5}$$

where:

K_{opt} – coefficient of optimal operation of wind turbine, which is given as:

$$K_{opt} = \frac{1}{2}\frac{C_{p\max}(\lambda_{opt},\beta)}{\lambda_{opt}^3}\rho\pi R^5 \tag{6}$$

where:

$C_{p\max}$ – maximum value of power coefficient at peak power point.

3. Model of Permanent Magnet Synchronous Generator

The dynamic equations of the three-phase Permanent Magnet Synchronous Generator (PMSG) can be expressed in synchronously rotating *dq* reference frame. The *d*-axis is aligned with the direction of the rotor flux vector and the *q*-axis is 90° ahead. The mathematical equations of the PMSG in *dq* frame can be described as follows [2–4, 8, 14, 15]:

$$v_{sd} = R_s i_{sd} + L_d \frac{d}{dt} i_{sd} - \omega_e L_q i_{sq} \tag{7}$$

$$v_{sq} = R_s i_{sq} + L_q \frac{d}{dt} i_{sq} + \omega_e L_d i_{sd} - \omega_e \psi_{PM} \tag{8}$$

$$\omega_e = n_p \cdot \omega_m \tag{9}$$

where:

v_{sd}, v_{sq} – components of the stator voltage vector in d and q axis,
i_{sd}, i_{sq} – components of the stator current vector in d and q axis,
L_d, L_q – stator inductances in direct and quadrature axis,
ψ_{PM} – flux linkage established by the permanent magnets,
R_s – stator phase resistance,
ω_e, ω_m – electrical and mechanical angular speed of the PMSG rotor,
n_p – number of pole pairs of PMSG.

The electromagnetic torque of PMSG can be expressed as follows:

$$T_e = \frac{3}{2} n_p [\psi_{PM} i_{sq} - (L_d - L_q) i_{sd} i_{sq}] \tag{10}$$

When the PMSG has a uniform air gap, then $L_d = L_q = L_s$ the simplified expression for the generator electromagnetic torque is given by:

$$T_e = \frac{3}{2} n_p \psi_{PM} i_{sq} \tag{11}$$

The mechanical equation of motion is given as:

$$T_t + T_e = J \cdot \frac{d}{dt} \omega_m + K_f \omega_m \tag{12}$$

where:

J – the total equivalent inertia,
K_f – coefficient of viscous friction.

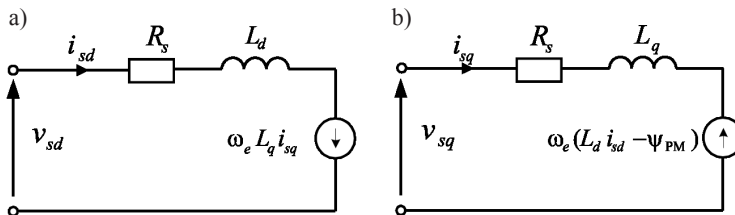The equivalent circuits of the PMSG have been presented in Figure 3.

Fig. 3. Equivalent circuits of the PMSG in *dq* frame: a) *d-axis* equivalent circuit,
b) *q-axis* equivalent circuit

4. MPPT and Pitch Angle Control

The objective of the Maximum Power Point Tracking (MPPT) algorithm is to maximize the power that the wind turbine can extract from the wind. This condition is achieved if the power coefficient of the wind turbine has a maximum value equal to $C_{p\max}$. In order to obtain the maximum power coefficient $C_{p\max}$ of the wind turbine, the tip speed ratio λ must be kept at optimum value λ_{opt} [1, 6, 15].

As shown in Fig. 4, the variable speed wind turbine systems with a pitch angle controller can be operated in four regions, determined by three specific wind speeds: cut-in wind speed, rated wind speed and cut-out wind speed [14, 15].
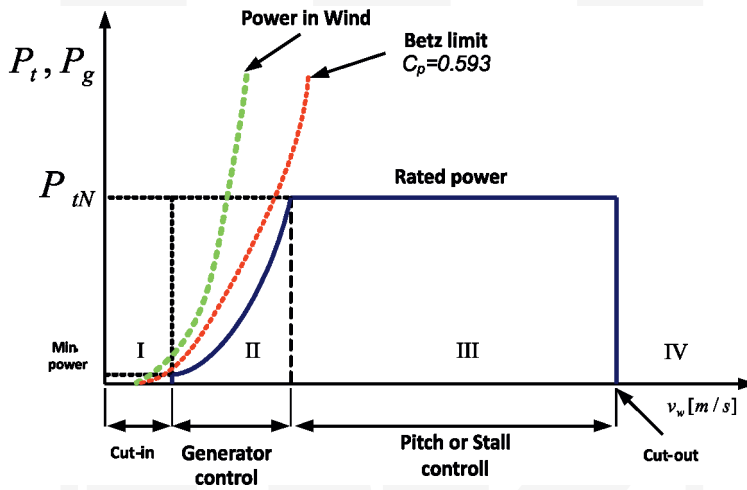

Fig. 4. Wind turbine mechanical power versus wind speed curve

The cut-in wind speed is the wind speed at which the wind turbine should capture enough power to start operation. The rated wind speed is the speed when the turbine produces nominal power. In the region of generator control, where the wind speeds are lower than the rated wind speed, the rotational speed of the PMSG is controlled at an optimal value, so that the maximum energy is extracted from the wind turbine. As the wind speed increases above the rated speed, the aerodynamic power control of the blades is required to keep the power at the rated value. This task is performed by using the pitch angle control or stall control [15]. The cut-out speed is the highest allowed wind speed at which turbine is allowed to operate.

In this article, the pitch angle control is considered for limitation of either the mechanical power generation or the turbine rotor speed, when these variables are overly high. When the wind speed exceeds the rated value the pitch angle controller should increase the angle of blades.

The schematic diagram of the blade pitch angle controller is shown in Fig. 5 [2, 14]. In the pitch angle controller, two control loops have been applied: the main control loop of wind turbine speed and the additional control loop of wind turbine power.
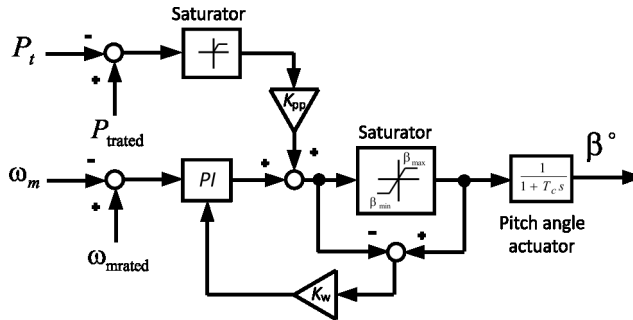
Fig. 5. Wind turbine pitch angle controller

In the main control loop, the rated speed ω_{mrated} of the wind turbine is compared with the measured rotor speed ω_m. In this loop, the PI controller with anti-windup has been applied. In the additional control loop, the rated turbine power P_{trated} is compared with the measured turbine power P_t. The output signal from the two control loops is added and designates the control signal of pitch angle actuator. The response speed of the pitch controller depends on the time constant of the pitch actuator.

5. Model of Control System of Machine Side Converter

Direct Torque Control (DTC) is an alternative to the Field Oriented Control (FOC) method in high performance applications due to its advantages [5, 8, 13, 16, 17]. The principle of DTC is based on directly selecting the appropriate stator voltage vectors according to the differences between the reference and the actual values of magnitude of the stator flux vector and electromagnetic torque.

The conventional DTC is implemented by using the hysteresis flux and torque controllers, which are operated with switching table. The alternative for control with the switching table is the implementation of DTC with Space Vector Modulation (DTC-SVM). The application of SVM ensures the lower harmonics of stator currents and allows to reduce the electromagnetic torque ripples. The other advantage of using SVM is the possibility of maintaining the constant switching frequency [8, 13, 16, 17].

Figure 6 shows the block scheme of the DTC-SVM system for control of PMSG with MSC. In the DTC-SVM control system, the PMSG is controlled on the basis of a proper selection of the stator voltage vector generated through the MSC converter. The control scheme of DTC-SVM consists of three control loops. The outer control loop with PI controller regulates the generator speed to follow the optimum speed ω_{opt}.

The two inner control loops with PI controllers regulate the magnitude of the stator flux vector and the electromagnetic torque of the PMSG. The magnitude of the stator flux vector ψ_s and the value of the electromagnetic torque T_e are compared with their reference values. Both error signals are sent to two PI controllers. The output control signals from PI controllers determine the reference values v_{sx}^* and v_{sy}^* of the stator voltage vector components of MSC.
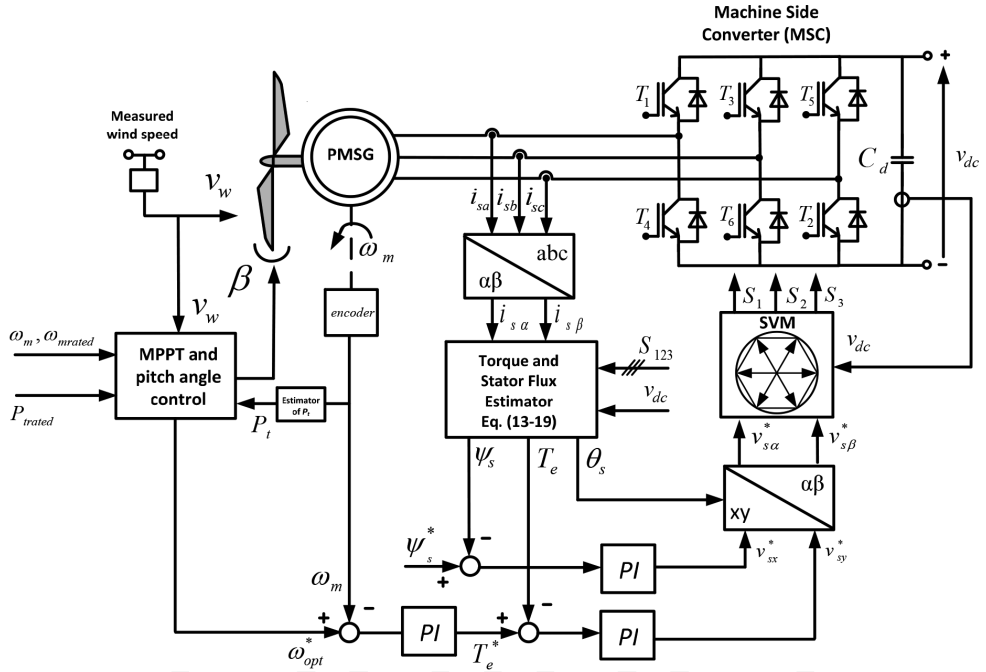
Fig. 6. Control diagram of DTC-SVM for Machine Side Converter

For an evaluation of the magnitude of the stator flux vector and the value of electromagnetic torque, several techniques have been presented in literature [13, 16]. In the strategy considered in this paper, the estimation block of stator flux vector ψ_s and electromagnetic torque T_e has been developed.

The components $\psi_{s\alpha}$, $\psi_{s\beta}$ of the stator flux vector are estimated by the equations [6, 16, 17]:

$$\psi_{s\alpha} = \int \left(v_{s\alpha} - R_s i_{s\alpha} \right) dt \tag{13}$$

$$\psi_{s\beta} = \int \left(v_{s\beta} - R_s i_{s\beta} \right) dt \tag{14}$$

where:

$\psi_{s\alpha}$, $\psi_{s\beta}$ – components of the stator flux vector in α-β system,
$v_{s\alpha}$, $v_{s\beta}$ – components of the stator voltage vector in α-β system,
$i_{s\alpha}$, $i_{s\beta}$ – components of the stator current vector in α-β system.

The application of integrators in the estimation block may cause problems with drifts and the determination of the initial values of the variable. This problem is especially significant when operating the generator at low speeds. The stator voltages are then quite small and the voltage drops on stator phase resistance are dominant. The method of dealing with this problem is the replacement of integrators by low-pass filters (LPF) [13].

The components $v_{s\alpha}$, $v_{s\beta}$ of the stator voltage vector can be determined by measuring DC link voltage v_{dc} and by using the information of the MSC switching states S_a, S_b, S_c as [2]:

$$v_{s\alpha} = \frac{v_{dc}}{3}\left(2S_a - S_b - S_c\right) \tag{15}$$

$$v_{s\beta} = \frac{v_{dc}}{\sqrt{3}}\left(S_b - S_c\right) \tag{16}$$

where:

S_a, S_b, S_c – switching states of the MSC,
v_{dc} – DC link voltage.

According to the components $\psi_{s\alpha}$, $\psi_{s\beta}$ of the stator voltage vector calculated from equation (13), (14), the magnitude and angle position of the stator flux vector can be determined as:

$$\psi_s = \sqrt{\psi_{s\alpha}^2 + \psi_{s\beta}^2} \tag{17}$$

$$\theta_s = \arctan\left(\frac{\psi_{s\beta}}{\psi_{s\alpha}}\right) \tag{18}$$

where:

θ_s – angle position of the stator flux-linkage vector.

The electromagnetic torque of the PMSG is estimated as follows:

$$T_e = \frac{3}{2}p_b\left(\psi_{s\alpha}i_{s\beta} - \psi_{s\beta}i_{s\alpha}\right) \tag{19}$$

6. Model of Control System of Grid Side Converter

The control objective for the Grid Side Converter (GSC) is to stabilize the DC-link voltage and to control the flow of the power delivered to the AC grid.

In the literature, one of the most commonly considered strategies is Voltage Oriented Control [1, 3–5, 15]. However, nowadays, the Direct Power Control method is developed [5, 9, 10]. The conventional DPC is based on controlling the instantaneous active and reactive power by selecting the proper voltage vector of the GSC converter based on the switching table. The DPC with hysteresis controllers and switching table generates the variable switching frequency.

In this paper, the control system of the GSC with the improved Direct Power Control Space Vector Modulation (DPC-SVM) method has been considered. The developed block scheme of the GSC control system is presented in Fig. 7. The DPC-SVM control is based on the instantaneous active and reactive power control loops. In order to obtain high power quality and to reduce the current harmonics in the output of the GSC, the LCL grid filter has been applied.

The control strategy of DPC-SVM is based on the instantaneous active and reactive power estimation as:

$$p_g = \frac{3}{2}\left(v_{g\alpha}i_{g\alpha} + v_{g\beta}i_{g\beta}\right) \tag{20}$$

$$q_g = \frac{3}{2}\left(v_{g\alpha}i_{g\beta} - v_{g\beta}i_{g\alpha}\right) \tag{21}$$

where:

$v_{g\alpha}, v_{g\beta}$ – components of the grid voltage vector in the stationary αβ frame,

$i_{g\alpha}, i_{g\beta}$ – components of the grid current vector in the stationary αβ frame.

In the DPC-SVM, three control loops with PI controllers have been used: the outer control loop and two inner control loops. The outer control loop with a PI controller is responsible for the control of the DC-link voltage between the MSC and the GSC converter. The reference DC-link voltage v_{dc}^* is compared with measured DC-link voltage v_{dc}. The output value from this PI controller is multiplied by the measured DC-link voltage v_{dc} and this value determines the reference value of the instantaneous active power p_g^*. For typical operation, the reference instantaneous reactive power is set to zero in order to obtain the unity power factor operation. The reference values of instantaneous active power p_g^* and reactive power q_g^* are compared with the measured values, calculated from equations (20, 21). The deviation of instantaneous active and reactive power are given to PI controllers. The output values from these controllers set the reference components v_{gd}^* and v_{gq}^* of the GSC voltage vector. This components are then transformed to the components $v_{g\alpha}^*$, $v_{g\beta}^*$ in stationary α-β system. The reference GSC voltage vector components $v_{g\alpha}^*$ and $v_{g\beta}^*$ are sent to the SVM block, which generates the required switching signals for the Grid Side Converter.

The angle positions θ_g of the grid voltage vector required for transformation to the α-β system is obtained from the Phase Locked Loop (PLL) block. The basic scheme of the PLL system is a feedback system with a PI regulator tracking the grid phase angle.
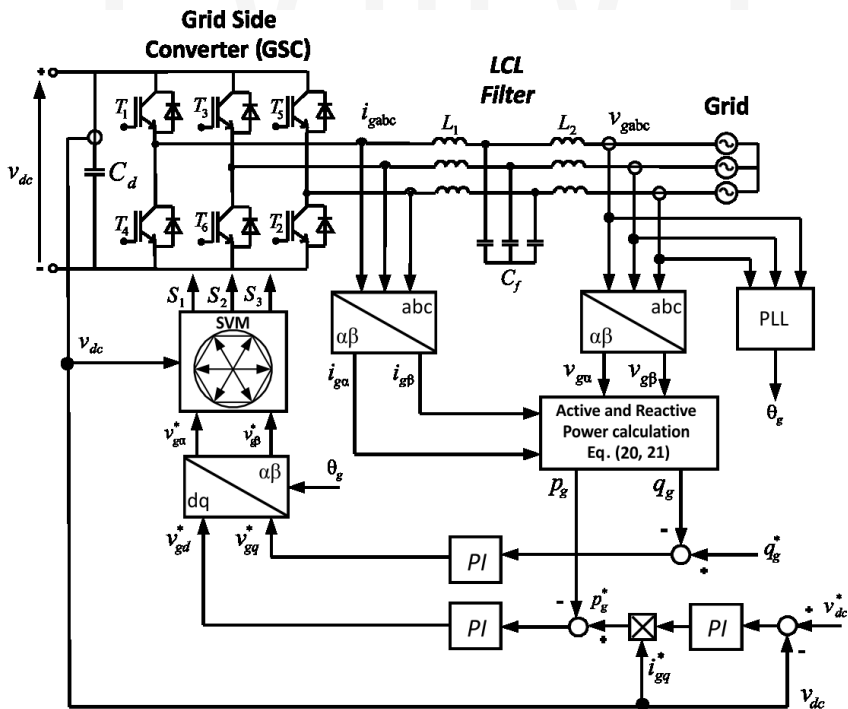

Fig. 7. Control diagram of DPC-SVM with LCL grid filter for the Grid Side Converter

7. LCL Grid Filter Design

In order to obtain high power quality and to reduce the current harmonics in the output of the GSC, the LCL grid filter has been used. In comparison to the conventional L grid filter, the LCL grid filter has better performance [7]. The LCL filter has the advantage of providing the proper decoupling between GSC and the AC grid.

The presented description of the LCL grid filter is based on the consideration of one phase circuit of a real three-phase filter. The equivalent scheme one phase circuit of LCL filter has been presented in Fig. 8 [7, 11, 12]:
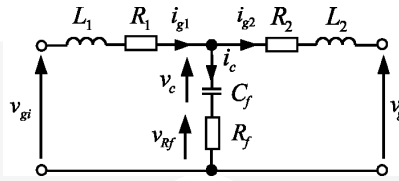
Fig. 8. Circuit diagram of one phase of LCL grid filter

where:

v_{gi} – the GSC output voltage,
v_g – the grid voltage,
L_1, R_1 – the filter inductance and resistance at the GSC side,
L_2, R_2 – the filter inductance and resistance at the grid side,
i_{g1} – the GSC output phase current,
i_{g2} – the grid phase current,
i_c – the filter capacitor current,
C_f, R_f – the filter capacitance and damping resistance,
v_C – the voltage of the filter capacitance.

The state equations of the LCL grid filter can be expressed in the form [7, 11]:

$$\frac{d}{dt}\begin{bmatrix} i_{g1} \\ i_{g2} \\ v_c \end{bmatrix} = \begin{bmatrix} -\dfrac{R_1+R_f}{L_1} & \dfrac{R_f}{L_1} & -\dfrac{1}{L_1} \\ \dfrac{R_f}{L_2} & \dfrac{R_2+R_d}{L_2} & \dfrac{1}{L_2} \\ \dfrac{1}{C_f} & -\dfrac{1}{C_f} & 0 \end{bmatrix}\begin{bmatrix} i_{g1} \\ i_{g2} \\ v_c \end{bmatrix} + \begin{bmatrix} \dfrac{1}{L_1} & 0 \\ 0 & -\dfrac{1}{L_2} \\ 0 & 0 \end{bmatrix}\begin{bmatrix} v_{gi} \\ v_g \end{bmatrix} \tag{22}$$

The design procedure of the LCL grid filter has been presented below [7, 11, 12].

The first step is the calculation of the base impedance Z_B, base inductance L_B, base capacitance C_B of the filter:

$$Z_B = \frac{V^2_{N(RMS)}}{S_N} \tag{23}$$

$$L_B = \frac{Z_B}{\omega_g} \tag{24}$$

$$C_B = \frac{1}{\omega_g Z_B} \tag{25}$$

where:

V_N – nominal phase converter voltage,

S_N – nominal apparent power of converter,

ω_g – the angular frequency of the grid.

The filter capacitance C_f is taken assuming that the filter capacitance should be less than 5% of the base capacitance C_B [7, 11].

$$C_f \leq 0.05 \cdot C_B \tag{26}$$

The magnitude of the current ripple $I_{maxrip}{}^{*}$ of the GSC output phase current can be selected between 10% and 25% of the nominal converter phase current I_N [7, 11]:

$$I_{max} = \sqrt{2}\left(0.1 \div 0.25\right) \cdot I_N \tag{27}$$

where:

$$I_N = \frac{S_N}{3V_N} \tag{28}$$

The filter inductance of the converter side L_1 and grid filter inductance L_2 can be calculated as:

$$L_1 = \frac{V_{dc}}{6 f_{sw} I_{max\,rip}} \tag{29}$$

$$L_2 = rL_1 \tag{30}$$

where:

f_{sw} – switching frequency of SVM of GSC,

V_{dc} – average DC link converter voltage,

r – designed ratio of the filter inductance L_2 to L_1 [12].

The LCL grid filter may cause voltage and current oscillations, which can increase the cut-off frequency of the filter. In order to cope with this problem, a damping resistor is added to the filter. Different circuits of the damping resistor connection are considered in literature [7, 12]. In this paper, the passive damping resistor R_f is added in series with the capacitor C_f. However, the damping resistance should not be too high because of the necessity to limit the power losses in the LCL grid filter.

The resistance of the damping can be calculated as:

$$R_f = \frac{1}{3 f_{res} C_f} \tag{31}$$

where:

f_{res} – is the resonant frequency, which can be calculated as:

$$f_{res} = \frac{1}{2\pi} \sqrt{\frac{L_1 + L_2}{L_1 L_2 C_f}} \tag{32}$$

In order to confirm the high performance of the LCL grid filter, the frequency responses should be determined. In this analysis, it is assumed that the AC grid is the ideal voltage source. Then, the transfer function H_{LCL} of the LCL grid filter considered as the ratio of grid current i_{g2} to voltage of GSC v_{gi} is described below [11, 12]:

$$H_{LCL}(s) = \frac{i_{g2}(s)}{v_{gi}(s)} = \frac{C_f R_f s + 1}{L_1 C_f L_2 s^3 + C_f (L_1 + L_2) R_f s^2 + (L_1 + L_2)s} \tag{33}$$

The frequency characteristics of the LCL grid filter without damping resistor and with damping resistor are shown in Fig. 9.
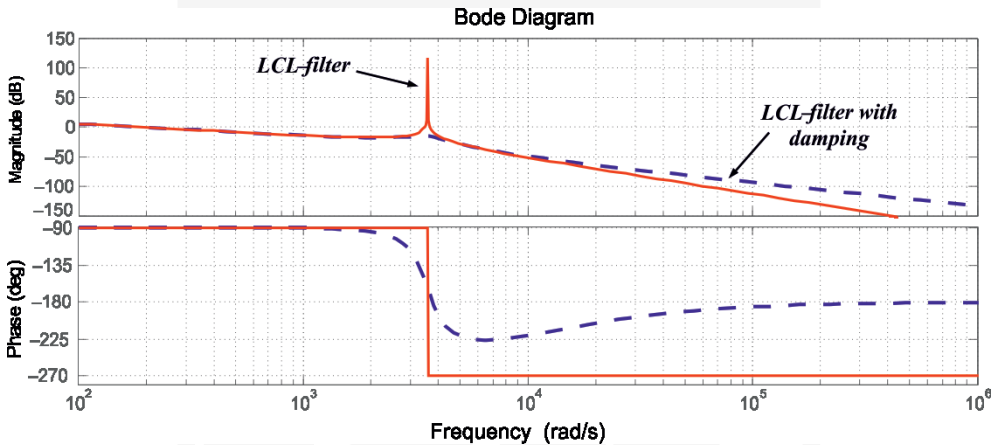
Fig. 9. Body diagram for transmittance of LCL grid filter without and with damping resistor

8. Simulation Results

In order to verify the effectiveness of the considered configuration and its control strategy, the digital simulation model has been developed in MATLAB/Simulink. Digital simulation studies made for the system with wind turbine parameters: rated power, P_t – 20 kW; rotor radius R – 4,4 m; maximum power coefficient C_{pmax} – 0.48; air density ρ – 1.225 kg/m³; 3-phase PMSG parameters: Rated power of PMSG P_g – 20 kW; stator dq-axis inductance $L_d = L_q = L_s$ – 4.48 mH; stator resistance R_s – 0.1764 Ω; number of pole pairs p_b – 18; rated speed Ω_N – 211 rpm; stator rated phase current I_{sn} – 35.1 A; LCL grid filter parameters: inductance of the GSC side L_1 – 4 mH; inductance of the grid side L_2 – 1 mH; damping resistance R_f – 1.5 Ω.

In order to evaluate the control system performance, simulations have been carried out based on the considered wind speeds variations, which are presented in Fig. 10. For the

simulated wind turbine model, the determined value of the optimal tip speed ratio λ_{opt} is equal to 8.1 and the maximum power coefficient C_{pmax} is equal to 0.48.

Figure 11 shows the waveforms of optimal ω_{opt} and the measured angular rotor speed ω_m of PMSG. It can be noticed that the generator speed ω_m is accurately adjusted to the waveform of the optimal speed. The reference angular rotor speed ω_{opt} is obtained from the MPPT algorithm. Moreover, the generator speed ω_m does not exceed the rated speed of the PMSG generator due to the response of the pitch angle algorithm.

The waveforms of the tip speed ratio λ and pitch angle β at various wind speeds have been presented in Fig. 12. From these waveforms, it can be noticed that the values of the tip speed ratio are kept at reference and maximum value ($\lambda = 8.1$) according to the operation of the MPPT algorithm. However, when wind speeds exceed the rated value ($v_w = 11$ m/s), the proper operation of the blade pitch angle controller can be noticed.
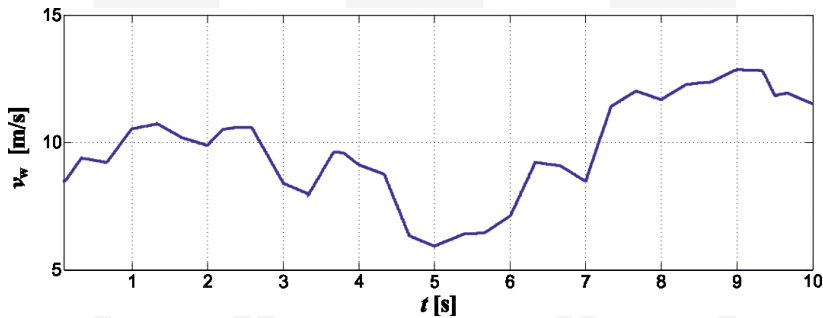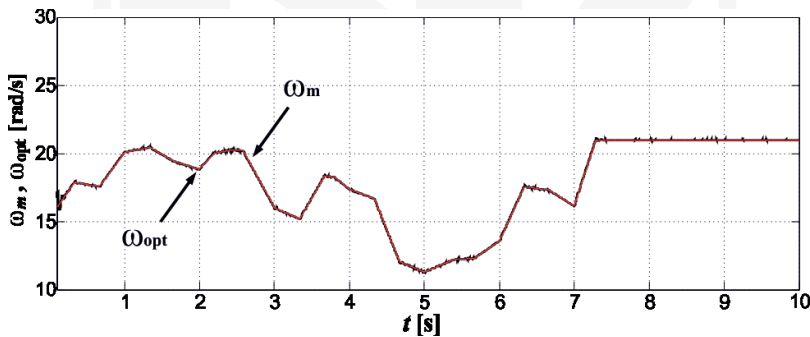

Fig. 10. Waveforms of wind speed v_w

Fig. 11. Waveforms of measured ω_m and reference speed ω_{opt} of PMSG

Figure 13 presents the waveform of the response of electromagnetic torque T_e of the PMSG. The time response of the electromagnetic torque of the PMSG have similar waveforms as the fast time variations of the wind speeds.

The trajectory of the stator flux vector has been presented in Fig. 14. From this Figure, it can be stated that the stator flux vector rotates with a constant magnitude and with small oscillation.
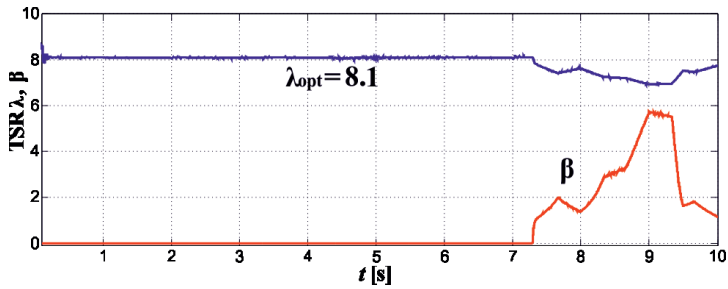
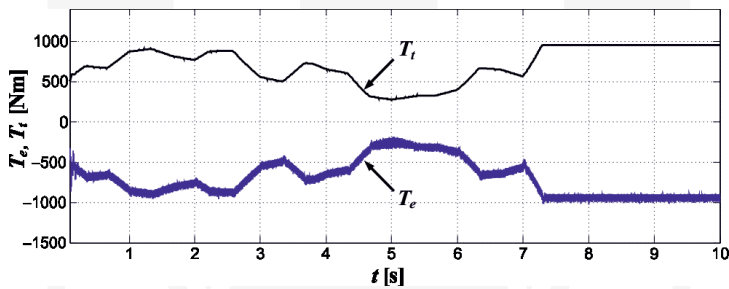Fig. 12. Waveforms of tip speed ratio λ and blade pitch angle β

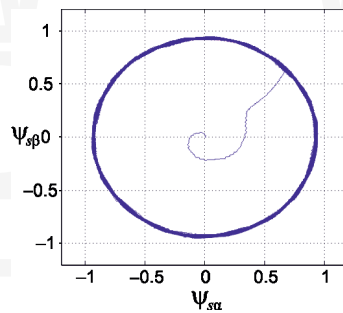Fig. 13. Waveform of electromagnetic torque T_e of PMSG

Fig. 14. Waveform trajectory of stator flux vector

The waveform of the DC-link voltage has been presented in Fig. 15. The instantaneous value of DC-link voltage is quite constant across a wide range of variations of the wind speed.

Figure 16 presents the waveforms of the grid side converter current before the LCL grid and grid phase current after the LCL grid filter. It can be stated that the high accuracy of the operation of the LCL grid filter is obtained.

Figure 17 shows the instantaneous active p_g and reactive power q_g delivered to the AC grid. The instantaneous reactive power q_g is set to zero in order to achieve the condition of unity power factor. The changes of instantaneous active power delivered to the AC grid are in accordance with the changes of the wind speeds.
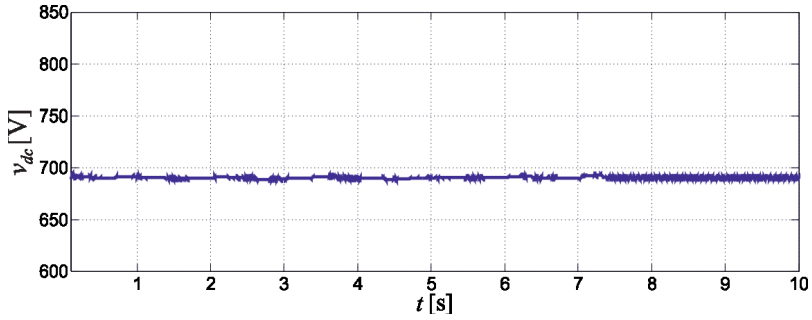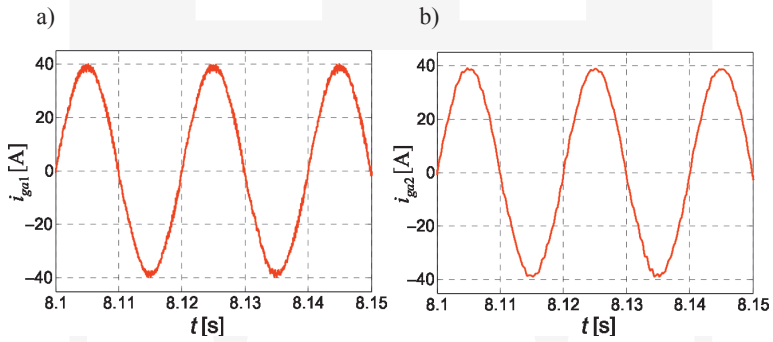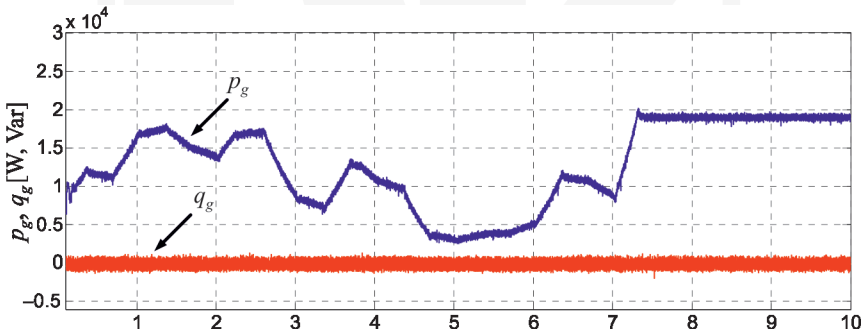
Fig. 15. Waveform of DC link voltage

a)   b)

Fig. 16. Waveforms of: a) converter phase current i_{ga1}, b) grid phase current i_{ga1}

Fig. 17. Waveforms of instantaneous active p_g and instantaneous reactive q_g grid power

9. Conclusions

In this paper, the dynamic modeling and the control structure of a wind energy conversion system with a direct-driven PMSG have been considered. High performance of the constantly switching frequency of the Direct Torque Control for the MSC and the Direct

Power Control for the GSC is presented. In the considered control method for a back-to-back converter system, the conventional hysteresis controllers and switching tables have been replaced by the Space Vector Modulation block.

The control strategy of MSC is based on enforcing the operation at the optimum values of rotor speed. The MPPT algorithm allows maintaining the maximum value of the optimal tip speed ratio and power coefficient as the result of wind speed variations. Additionally, the pitch angle control scheme is proposed to achieve a limitation of the maximum turbine power and to prevent mechanical damage of the wind turbine.

The performance of the wind energy conversion system with the LCL grid filter has been studied and verified by digital simulations. The conducted simulation results confirm the high performance and good properties of the considered DTC and DPC of the wind energy conversion system. The simulation results also demonstrate the correct operation and high efficiency of the LCL grid filter.

References

[1] Cernelic J., Stumberger S., Dolinar D., *Control for Grid Connected Small Wind Turbine System*, Przegląd Elektrotechniczny, R. 91, Nr 5/2015, 174–178.

[2] Errami Y., Ouassaid M., Cherkaoui M., Maaroufi M., *Variable Structure Sliding Mode Control and Direct Torque Control of Wind Power Generation System Based on the PM Synchronous Generator,* Journal of Electrical Engineering, Vol. 66, No. 3, 2015, 121–131.

[3] Gajewski P., Pieńkowski K., C*ontrol of a Variable Speed Wind Turbine System with PMSG Generator*, Maszyny Elektryczne – Zeszyty Problemowe, Nr. 3, 2015, 75–90.

[4] Gajewski P., Pieńkowski K., *Analysis of a Wind Energy Converter System with PMSG Generator*, Technical Transactions 1-E/2015, 219–228.

[5] Hasnaoui B.K.O., Allaqui M., Belhadj J., *PMSG Gear-Less Wind Turbine Equipped with an Active and Reactive Power Supervisory*, International Journal of Renewable Energy Research, Vol. 4, No. 2, 2014, 435–444.

[6] Innoue Y., Morimoto S., Sanada M., *Control Method for Direct Torque Controlled PMSG in Wind Power Generation System*, International Electric Machines and Drives Conference, IEMDC'09, 2009, 1231–1238.

[7] Liserre M., Blaabjerg F., Hansen S., *Design and Control of an LCL-Filter-Based Three-Phase Active Rectifier*, IEEE Transaction on Industry Applications, Vol. 41, No. 5, 2005, 1281–1291.

[8] Magesh M., Sundareswaran R., *PMSG Based Wind Energy Conversion with Space Vector Modulation*, International Journal of Energy and Power Engineering, Vol. 4, No. 3, 2015, 146–152.

[9] Malinowski M., Jasiński M., Kaźmierkowski M.P., *Simple Direct Power Control of Three-Phase PWM Rectifier Using Space-Vector Modulation (DPC-SVM)*, IEEE Transaction on Industrial Electronics, Vol. 51, 2004, 447–454.

[10] Milczarek A., Malinowski M., *Monitoring and Control Algorithm Applied to Small Wind turbine Grid-Connected/Stand-Alone Mode of Operation*, Przegląd Elektrotechniczny, R. 88, Nr 12a, 2012, 18–22.

[11] Renzhong X., Lie X., Junjun Z., Jie D., *Design and Research on the LCL Filter in Three-Phase PV Grid-Connected Inverters*, International Journal of Computer and Electrical Engineering, Vol. 5, No. 3, 2013, 322–325.

[12] Reznik A., Simoes M.G., Al-duraa A., Muyeen S.M., *LCL Filter Design and Performance Analysis for Grid Interconnected System*, IEEE Transactions on Industry Applications, Vol. 50, No. 2, 2014, 1225–1232.

[13] Swierczyński D., *Direct Torque Control with Space Vector Modulation (DTC-SVM) of Inverter-fed Permanent Magnet Synchronous Motor Drive,* Ph.D. Thesis, Warsaw University of Technology, 2005.

[14] Wang Y., Hai R., *Power Control of Permanent Magnet Synchronous Generator Direct Driven by Wind Turbine,* International Journal of Signal Processing System, Vol. 1, No. 2, 2013, 244–249.

[15] Wu B., Yongqiang L., Navid Z., Samir K., *Power Conversion and Control of Wind Energy*, John Wiley & Sons, INP., Publication 2011.

[16] Xu Z., Rahman M.F., *Direct Torque and Flux Regulation of an IPM Synchronous Motor Drive Using Variable Structure Control Approach*, IEEE Transactions on Power Electronics, Vol. 22, No. 6, 2007, 2487–2498.

[17] Zhang J., Rahman M.F., Grantham C., *A New Scheme to Direct Torque Control of Interior Permanent Magnet Synchronous Machine Drives for Constant Inverter Switching Frequency and Low Torque Ripple*, Power Electronics and Motion Control Conference IPEMC, CES/IEEE 5th, 2006, 1–5.